Open access • Journal Article • DOI:10.1002/2014GL062964

Plasmatrough exohiss waves observed by Van Allen Probes: Evidence for leakage from plasmasphere and resonant scattering of radiation belt electrons

Hui Zhu, Zhenpeng Su, Zhenpeng Su, Fuliang Xiao ...+14 more authors

Institutions: University of Science and Technology of China, Chinese Academy of Sciences, Changsha University of Science and Technology, University of Iowa ...+4 more institutions

Published on: 28 Feb 2015 - Geophysical Research Letters (John Wiley & Sons, Ltd)

Topics: Plasmasphere, Van Allen radiation belt, Van Allen Probes and Hiss

2-2015

Plasmatrough exohiss waves observed by Van Allen Probes: Evidence for leakage from plasmasphere and resonant scattering of radiation belt electrons

Hui Zhu
University of Science and Technology of China

Zhenpeng Su
University of Science and Technology of China

Fuliang Xiao
Changsha University of Science and Technology

Huinan Zheng
University of Science and Technology of China

Yuming Wang
University of Science and Technology of China

See next page for additional authors

Recommended Citation

H. Zhu, Z. Su, F. Xiao, H. Zheng, Y. Wang, C. Shen, T. Xian, S. Wang, C. A. Kletzing, W. S. Kurth, G. B. Hospodarsky, H. E. Spence, G. D. Reeves, H. O. Funsten, J. B. Blake, and D. N. Baker, 'Plasmatrough exohiss waves observed by Van Allen Probes: Evidence for leakage from plasmasphere and resonant scattering of radiation belt electrons', Geophysical Research Letters, vol. 42, no. 4, pp. 1012–1019, Feb. 2015.

AGU PUBLICATIONS

Geophysical Research Letters

RESEARCH LETTER
10.1002/2014GL062964

Key Points:
- Exohiss observed by Van Allen Probes in the low-latitude plasmatrough
- Observational evidence for leakage of hiss from plasmasphere to plasmatrough
- Strong scattering loss effect of exohiss on radiation belt electrons

Correspondence to:
Z. Su,
szpe@mail.ustc.edu.cn

Citation:
Zhu, H., et al. (2015), Plasmatrough exohiss waves observed by Van Allen Probes: Evidence for leakage from plasmasphere and resonant scattering of radiation belt electrons, *Geophys. Res. Lett.*, *42*, 1012–1019, doi:10.1002/2014GL062964.

Received 23 DEC 2014
Accepted 29 JAN 2015
Accepted article online 2 FEB 2015
Published online 26 FEB 2015

Plasmatrough exohiss waves observed by Van Allen Probes: Evidence for leakage from plasmasphere and resonant scattering of radiation belt electrons

Hui Zhu[1,2,3,4], Zhenpeng Su[1,2,4], Fuliang Xiao[5], Huinan Zheng[1,2,4], Yuming Wang[1,4], Chao Shen[6], Tao Xian[7], Shui Wang[1], C. A. Kletzing[8], W. S. Kurth[8], G. B. Hospodarsky[8], H. E. Spence[9], G. D. Reeves[10], H. O. Funsten[11], J. B. Blake[12], and D. N. Baker[13]

[1]CAS Key Laboratory of Geospace Environment, Department of Geophysics and Planetary Sciences, University of Science and Technology of China, Hefei, China, [2]State Key Laboratory of Space Weather, Chinese Academy of Sciences, Beijing, China, [3]Mengcheng National Geophysical Observatory, School of Earth and Space Sciences, University of Science and Technology of China, Hefei, China, [4]Collaborative Innovation Center of Astronautical Science and Technology, Harbin, China, [5]School of Physics and Electronic Sciences, Changsha University of Science and Technology, Changsha, China, [6]State Key Laboratory of Space Weather, Center for Space Science and Applied Research, Chinese Academy of Sciences, Beijing, China, [7]Key Laboratory of the Atmospheric Composition and Optical Radiation, CAS, School of Earth and Space Sciences, University of Science and Technology of China, Hefei, China, [8]Department of Physics and Astronomy, University of Iowa, Iowa City, Iowa, USA, [9]Institute for the Study of Earth, Oceans, and Space, University of New Hampshire, Durham, New Hampshire, USA, [10]Space Science and Applications Group, Los Alamos National Laboratory, Los Alamos, New Mexico, USA, [11]ISR Division, Los Alamos National Laboratory, Los Alamos, New Mexico, USA, [12]The Aerospace Corporation, Los Angeles, California, USA, [13]Laboratory for Atmospheric and Space Physics, University of Colorado Boulder, Boulder, Colorado, USA

Abstract Exohiss waves are whistler mode hiss observed in the plasmatrough region. We present a case study of exohiss waves and the corresponding background plasma distributions observed by the Van Allen Probes in the dayside low-latitude region. The analysis of wave Poynting fluxes, suprathermal electron fluxes, and cold electron densities supports the scenario that exohiss leaks from the plasmasphere into the plasmatrough. Quasilinear calculations further reveal that exohiss can potentially cause the resonant scattering loss of radiation belt electrons ~<MeV on a comparable time scale to that associated with the storm time plasmaspheric hiss. These results clearly illustrate that exohiss may need to be taken into account in future radiation belt models.

1. Introduction

Whistler mode hiss is an important and common type of electromagnetic wave with typical frequency ranging between ~100 Hz and ~2000 Hz in the terrestrial inner magnetosphere [*Thorne et al.*, 1973; *Meredith et al.*, 2004]. Hiss waves in the high-density plasmasphere or the dayside plasmaspheric plume are usually referred to as plasmaspheric hiss [*Thorne et al.*, 1973]. Plasmaspheric hiss can produce effective pitch angle scattering of energetic electrons via cyclotron resonance, responsible for the formation of the slot region ($2 < L < 3$) between the inner and outer radiation belts [*Lyons and Thorne*, 1973; *Abel and Thorne*, 1998a, 1998b] and the slow decay of outer belt electrons [*Summers et al.*, 2008; *Thorne et al.*, 2013; *Li et al.*, 2014; *Ni et al.*, 2014]. Various generation mechanisms of plasmaspheric hiss have been proposed over the past several decades. One important candidate is the electron cyclotron resonance instability inside the plasmasphere [*Thorne et al.*, 1979; *Church and Thorne*, 1983; *Cornilleau-Wehrlin et al.*, 1985; *Li et al.*, 2013]. The other candidates are considered to be the external sources, e.g., lightning-generated whistlers [*Sonwalkar and Inan*, 1989; *Green et al.*, 2005; *Meredith et al.*, 2006] and whistler mode chorus waves outside the plasmasphere [*Bortnik et al.*, 2008, 2009; *Chen et al.*, 2012a, 2012b]. Recently, the fine structures of plasmaspheric hiss have been presented by *Summers et al.* [2014], allowing a further reanalysis of its generation mechanism.

Hiss waves outside the plasmasphere, reported in the early works [*Russell et al.*, 1969; *Thorne et al.*, 1973], are referred to as exohiss [*Thorne et al.*, 1973]. Considering that exohiss was primarily observed in the dayside high-latitude ($\lambda > 35°$) region, *Thorne et al.* [1973] interpreted exohiss as the leakage of plasmaspheric hiss in the presence of weak density gradient around the plasmapause. Such leakage of hiss waves from plasmasphere to plasmatrough has been further reproduced by full lifetime ray tracing simulations

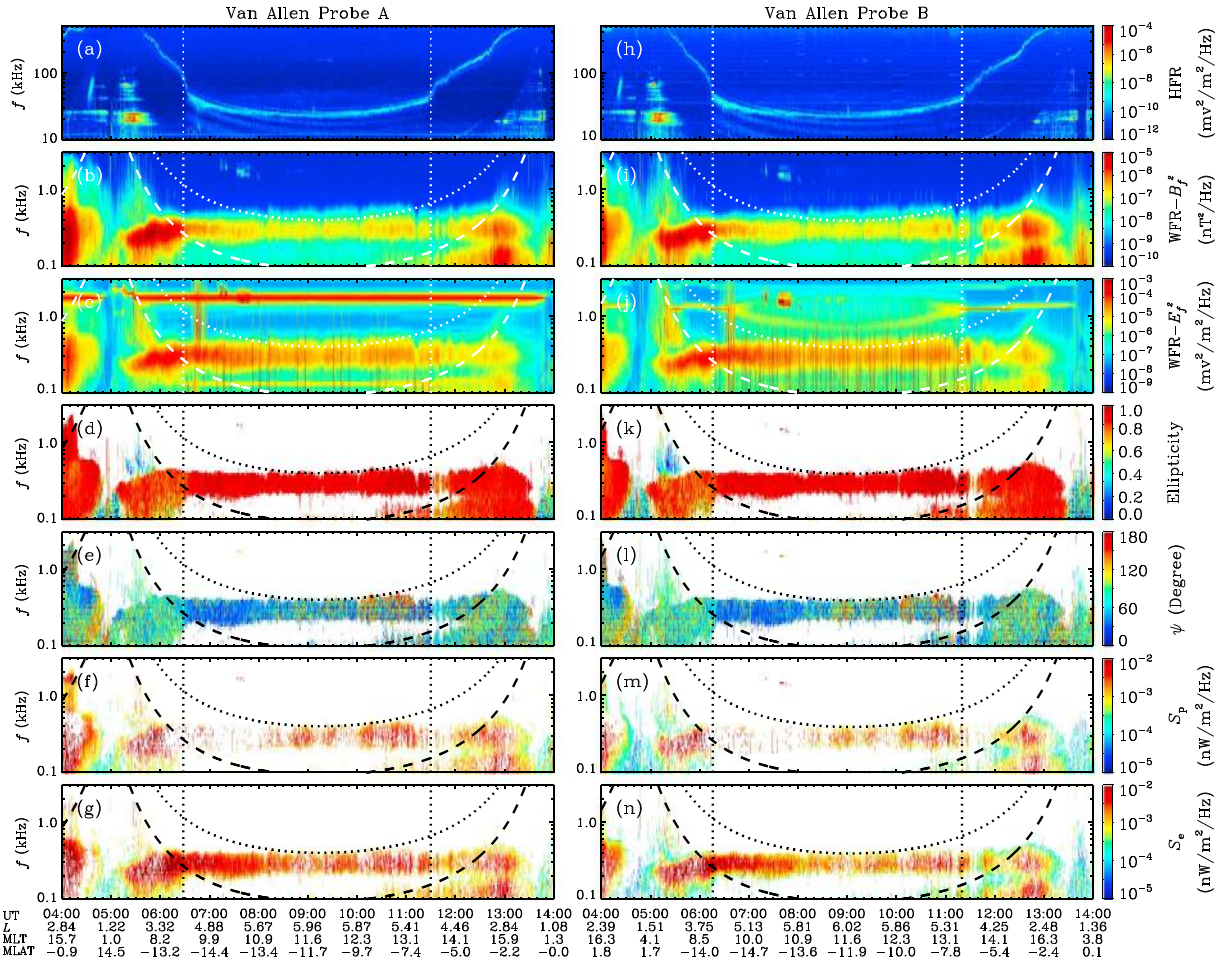

Figure 1. (a and h) Frequency-time spectrograms of electric power spectral density in the HFR channel; (b and i) magnetic and (c and j) electric power spectral density in the WFR channel; (d and k) the ellipticity of magnetic field polarization; (e and l) normal angle ψ; (f and m) poleward propagating Poynting fluxes S_p and (g and n) equatorward propagating Poynting fluxes S_e. The vertical lines denote the plasmapause location. The dotted and dashed curves (in Figures 1b–1g and 1i–1n) indicate $0.1f_{ce}$ and lower hybrid resonance frequency f_{lhr}.

[*Bortnik et al.*, 2008]. So far, however, there has been no direct observational evidence for the origin of exohiss. In this study, we report an exohiss wave event detected by the Van Allen Probes [*Mauk et al.*, 2013] in the low-latitude region ($|\lambda| < 15°$) on 2 March 2014 and analyze the wave propagation characteristics and the corresponding background plasma distribution to provide some observational evidence for the leakage of hiss waves from plasmasphere to plasmatrough. Moreover, we calculate the quasilinear diffusion coefficients of energetic electrons for the cyclotron/Landau resonance with observed exohiss and emphasize the potential loss effect of exohiss on radiation belt electrons.

2. Event Overview

Figure 1 gives an overview of the event observed by the waves instrument of the Electric and Magnetic Field Instrument Suite and Integrated Science (EMFISIS) suite [*Kletzing et al.*, 2013] on board Van Allen Probes during 04:00–14:00 UT on 2 March 2014. The upper hybrid resonance bands (bright lines) can be clearly identified in the electric power spectral density of the High-Frequency Receiver (HFR) (Figures 1a and 1h). The jump in density at the plasmapause, corresponding to the jump of upper hybrid resonance band, was detected by Van Allen Probe A around 06:28 UT ($L = 4.1$, MLAT $= -14.3°$, and MLT = 9.1) in the outbound pass or 11:30 UT ($L = 5.0$, MLAT $= -6.2°$, and MLT = 13.5) in the inbound pass, and by Van Allen Probe B around 06:16 UT ($L = 4.2$, MLAT $= -14.6°$, and MLT $= 9.0$) in the outbound pass or 11:20 UT ($L = 5.0$, MLAT $= -7.0°$, and MLT $= 13.4$) in the inbound pass. The plasmaspheric hiss and exohiss were observed by the Waveform Receiver (WFR) (Figures 1b, 1c, 1i, and 1j) inside and outside of

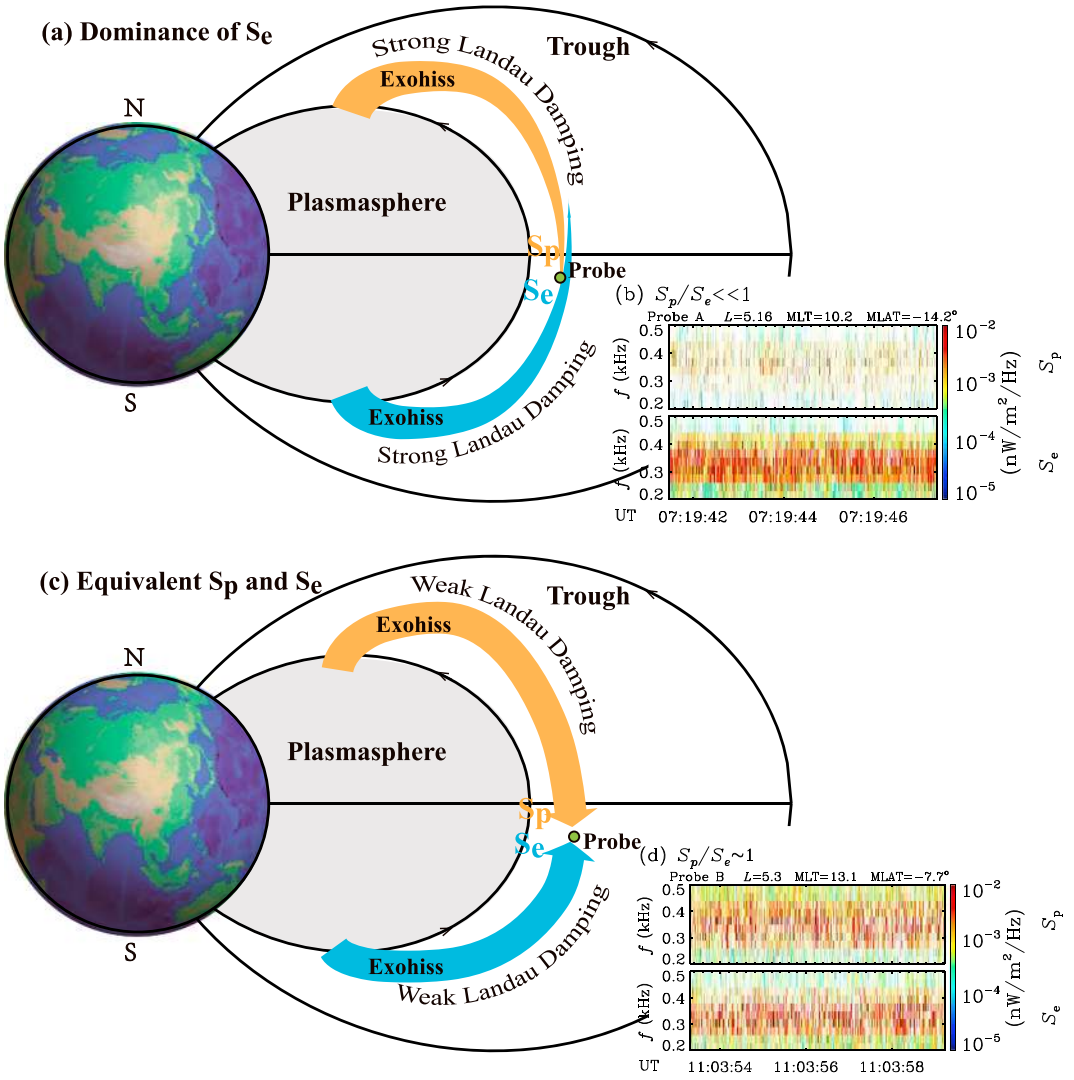

Figure 2. A schematic representation of exohiss with two snapshots of equatorward and poleward Poynting fluxes from waveform-continuous-burst mode data. The grey region represents the high-density plasmasphere, and the green points indicate the probe locations in the Southern Hemisphere. The arrows represent the leaked exohiss waves, and the arrow width represents the wave intensity.

plasmapause, respectively. Their corresponding normal angle ψ (Figures 1e and 1l) and Poynting fluxes (Figures 1f, 1g, 1m, and 1n) were determined via singular value decomposition method [*Santolik et al.*, 2003]. Exohiss occurred in the same frequency range as plasmaspheric hiss, but had weaker intensity. Both types of waves are predominantly circularly polarized with ellipticity close to 1. For plasmaspheric hiss, the equatorward propagating ($\psi < 90°$) components S_e and poleward propagating ($\psi > 90°$) components S_p of Poynting fluxes simultaneously existed with approximately equivalent intensities, implying the bounce propagation of plasmaspheric hiss. In contrast, there existed two distinct spatial regions for exohiss: (1) the prenoon sector (roughly corresponding to the outbound pass) with the dominance of S_e, and (2) the afternoon sector (roughly corresponding to the inbound pass) with the nearly equivalent S_e and S_p. Note that here S_p and S_e represent the absolute intensities of Poynting flux rather than the parallel/antiparallel components with respect to the magnetic field.

3. Evidence for Leakage From Plasmasphere

Plasmaspheric hiss is usually trapped in the high-density plasmasphere, experiencing magnetospheric reflection and plasmapause reflection [*Bortnik et al.*, 2008]. If the angle between wave normal and

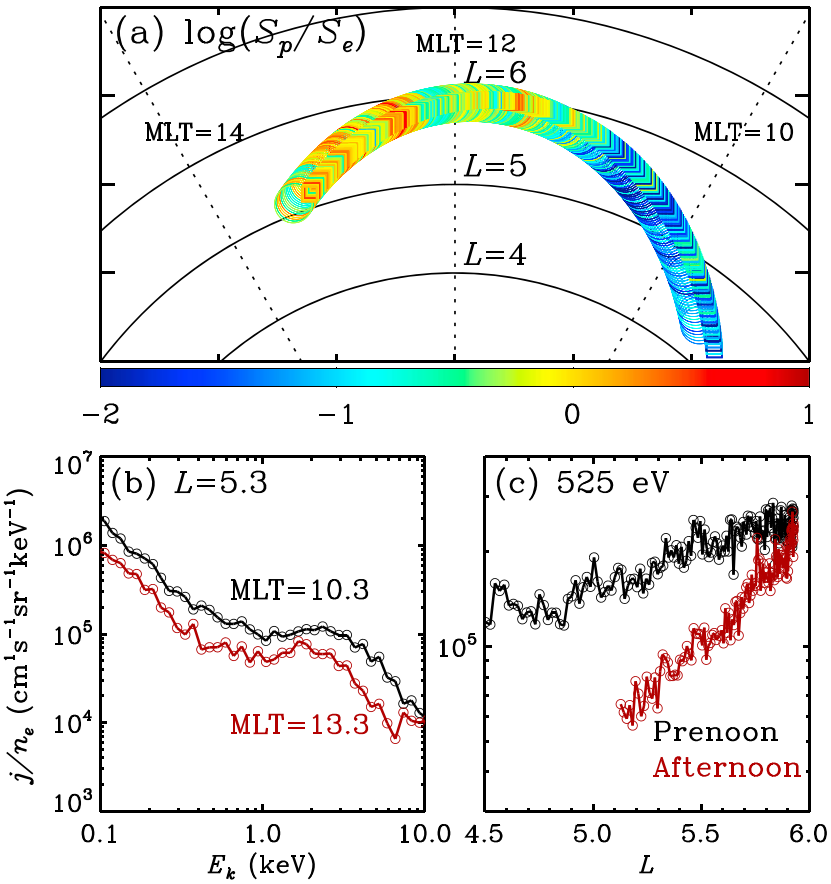

Figure 3. (a) The values of log(S_p/S_e) on the *L*-MLT plane; (b) j/n_e as a function of E_k for the prenoon and afternoon sectors; (c) j/n_e as a function of *L* at E_k = 525 eV. In Figure 3a, the circle and square symbols represent the data from Van Allen Probes A and B, respectively.

plasmapause normal is not large enough (do not satisfy total reflection condition), the hiss waves will pass across the plasmapause into the trough without reflection and then evolve into the so-called exohiss [*Bortnik et al.*, 2008]. These leaked hiss waves propagate toward the equator and undergo Landau damping by suprathermal (0.1–10 keV) electrons [*Bortnik et al.*, 2006, 2007; *Li et al.*, 2010]. If hiss waves are leaked relatively symmetrically from both the Northern and Southern Hemispheres of the plasmasphere, we can expect three types of observations in the low-latitude plasmatrough: (1) no exohiss waves; (2) the dominance of equatorward Poynting fluxes; (3) the occurrence of roughly equivalent equatorward and poleward Poynting fluxes. For the first type, exohiss from both hemispheres suffers too strong Landau damping to reach the low-latitude region. For the second type (see Figure 2a), if the observation point is far enough away from the equator accompanied by relatively strong Landau damping, the observed equatorward Poynting fluxes S_e (undergoing shorter damping period) can dominate over the poleward ones S_p ($S_p/S_e << 1$). For the last type (see Figure 2b), the waves from both hemispheres suffer relatively weak and comparable Landau damping and can reach the low-latitude region with similar Poynting fluxes in both directions ($S_p/S_e \sim 1$). As shown in Figure 3a, the Poynting flux observations fit the second type of expectation ($S_p/S_e << 1$) in the prenoon sector while they fit the third type of expectation ($S_p/S_e \sim 1$) in the afternoon sector. In view of the insignificant variation of the observation latitudes, the change in Landau damping efficiency can be expected to cause the change in the Poynting flux ratio S_p/S_e. In general, the Landau damping efficiency is proportional to the suprathermal electron (0.1–10 keV) number density but inversely proportional to the cold electron number density. Here the suprathermal electron fluxes *j* were provided by the Helium, Oxygen, Proton, and Electron (HOPE) Mass Spectrometer [*Funsten et al.*, 2013] on board the Van Allen Probes, and the cold electron number density n_e was derived from the upper hybrid resonance frequency f_{uhf} observed by the HFR instrument. Figure 3b shows a representative comparison of j/n_e at the same L = 5.3 but different MLT = 10.3 (in the prenoon sector) and 13.3 (in the afternoon sector).

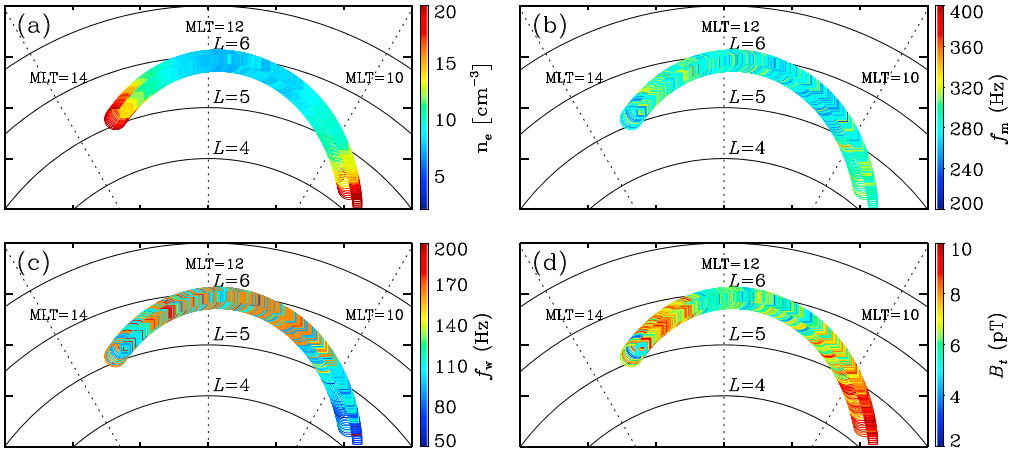

Figure 4. (a) Electron number densities n_e, (b) central frequency f_m, (c) frequency bandwidth f_w, and (d) wave amplitudes B_t on the L-MLT plane. The circle and square symbols represent the data from Van Allen Probes A and B, respectively.

Figure 3c gives the comparison of j/n_e observed in the prenoon and afternoon sectors at a fixed energy $E_k = 525$ eV. Obviously, observed values of j/n_e in the prenoon sector were up to 5 times larger than those in the afternoon sector (generally consistent with the previous statistical results) [*Bortnik et al.*, 2007; *Li et al.*, 2010]. This provides strong evidence that Poynting flux ratio S_p/S_e is controlled by the strength of Landau damping. The present observations support the previously proposed scenario that exohiss originates from plasmaspheric hiss.

4. Resonant Scattering of Radiation Belt Electrons

Quasilinear theory is widely used to quantitatively describe wave-particle interaction [e.g., *Horne et al.*, 2005; *Glauert and Horne*, 2005; *Summers*, 2005; *Shprits and Ni*, 2009; *Su et al.*, 2010]. Using the storm time evolution of electron radiation belt (STEERB) code [*Su et al.*, 2010, 2014], we calculate here the bounce-averaged diffusion coefficients of radiation belt electrons driven by exohiss in the typical dipole geomagnetic field.

The HFR-observed upper hybrid resonance line f_{uhf} is used to derive the cold electron density, and the WFR-observed magnetic power spectral density of exohiss is assumed to obey the Gaussian distribution with the center f_m, half-width f_w, and amplitude B_t. Figure 4 shows the derived electron number densities and wave distribution parameters with the time resolution of 1 min in the L-MLT plane. The results obtained from Van Allen Probe A were generally consistent with those obtained from Van Allen Probe B. All of

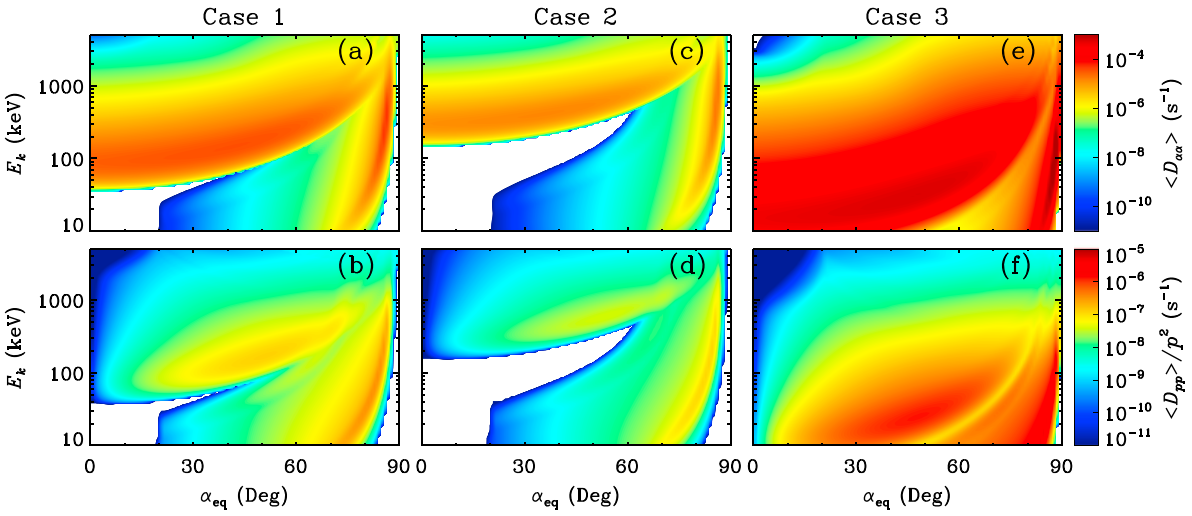

Figure 5. Bounce-averaged diffusion rates in (a, c, and e) pitch angle $\langle D_{\alpha\alpha}\rangle$ and (b, d, and f) momentum $\langle D_{pp}\rangle/p^2$ as functions of equatorial pitch angle α_{eq} and kinetic energy E_k for the three cases listed in Table 1.

Table 1. The Input Parameters for the Calculation of Quasilinear Diffusion Coefficients[a]

Case	L	n_{e0} (cm^{-3})	f_{pe}/f_{ce}	f_m (Hz)	f_w (Hz)	f_1 (Hz)	f_2 (Hz)	B_t (pT)
1	6	6.73	5.76	300	150	75	525	10
2	5	9.08	3.87	300	150	75	525	10
3	5	136.2	15	500	300	100	2000	50

[a]The term n_{e0} is the equatorial electron density, which is mapped from the local electron density n_e in Figure 3 , according to $n_e = n_{e0}(\cos\lambda)^{-2\nu}$ with $\nu = 3$ [*Denton et al.*, 2002] in Cases 1 and 2. In Case 3, n_{e0} is taken as a typical number density inside plasmasphere, and ν is assumed to 3. The term f_{pe} is the equatorial electron plasma frequency, and f_{ce} is the equatorial electron gyrofrequency.

the number densities n_e were smaller than 20 cm^{-3}, confirming the location of Van Allen Probes in the plasmatrough. The central frequencies gathered around 300 Hz with bandwidths varying between 50 Hz and 150 Hz. The maximum amplitude was 10.8 pT, and the mean amplitude was about 6.7 pT. Obviously, the amplitude of exohiss was nearly an order of magnitude smaller than that of the typical storm time plasmaspheric hiss ~50–100 pT [*Meredith et al.*, 2004].

Figure 5 shows three examples of diffusion coefficients with the input parameters listed in Table 1. The first two cases correspond to the exohiss with the electron density and wave parameters observed at $L = 6$ and 5, while the third case corresponds to the typical storm time plasmaspheric hiss [*Ni et al.*, 2013, 2014]. In all the three cases, the tangent of wave normal angle $X = \tan\psi$ is assumed to obey the typical Gaussian distribution with the center $X_m = 0$, half-width $X_w = 0.577$, lower $X_1 = 0$, and upper $X_2 = 1$ limits, and these waves are further assumed to be distributed in the latitude range $|\lambda| \leq 40°$ with fixed frequency and wave normal angle distributions. The maximum number of cyclotron resonance for low frequency whistler mode waves is generally determined by the particle momentum p, wave frequency f, the ratio f_{pe}/f_{ce}, and the normal angle ψ [*Mourenas and Ripoll*, 2012]. For the present three cases, the obtained maximum numbers of cyclotron resonance $|N|$ are 12, 7, and 30, respectively. Hence, without loss of consistency, the contributions of cyclotron resonances ($N = \pm1, \pm2, \ldots, \pm30$ orders) and Landau resonance ($N = 0$ order) are taken into account for all three cases.

The minimum cyclotron-resonant energies of exohiss are ~> 40 keV, much higher than those of plamaspheric hiss (primarily due to the change in f_{pe}/f_{ce}). The Landau resonance of both types of waves mainly occurs at the large equatorial pitch angles (close to 90°) for high energy (~> 100 keV) electrons and extends to smaller pitch angles for low energy (~< 100 keV) electrons. At the energies ~< MeV (depending the location L), the exohiss-driven pitch angle diffusion rates peak near the loss cone, while the corresponding momentum diffusion rates gradually vanish as the pitch angle decreases, suggesting that exohiss can cause the precipitation loss of radiation belt ~< MeV electrons. Interestingly, compared to plasmaspheric hiss, exohiss with a much smaller wave amplitude has the comparable scattering effect ($\langle D_{\alpha\alpha}\rangle \sim 5\times10^{-5}$ s^{-1}) on the energetic (100–400 keV) electrons near the loss cone. It should be mentioned that, we have performed more test calculations (not shown for brevity) and found no significant sensitivity of diffusion coefficients to the background density, frequency, and normal angle distributions.

5. Summary

We report an event of exohiss observed by Van Allen Probes in the dayside ($9 < \mathrm{MLT} < 14$) low-latitude ($-15° < \lambda < -6°$) plasmatrough ($4 < L < 6$) region. The exohiss appeared as a frequency-steady broadband whistler mode emission with circular polarization. The wave spectra peaked around 300 Hz with the amplitude up to 10.8 pT.

We analyze the wave propagation characteristics and the corresponding background plasma distribution. The wave Poynting fluxes were dominated by the equatorward propagating components in the prenoon sector but consisted of two equivalent equatorward and poleward propagating components in the afternoon sector. Moreover, the ratios of suprathermal electron fluxes to the cold electron densities j/n_e in the prenoon sector were up to 5 times larger than those in the afternoon sector. These observations support the previously proposed scenario that exohiss is the leaked plasmaspheric hiss from the plasmasphere into the plasmatrough. The leaked hiss experiences Landau damping with different efficiencies in the prenoon and afternoon sector. The large j/n_e produces stronger Landau damping and consequently the dominance

of equatorward Poynting fluxes (undergoing a shorter damping period) in the low-latitude region. In contrast, the small j/n_e yields weaker Landau damping and consequently the equivalence of equatorward and poleward Poynting fluxes.

We further calculate the bounce-averaged diffusion coefficients of radiation belt electrons due to cyclotron/Landau resonance with the observed exohiss. For ~< MeV electrons, the pitch angle diffusion rates behave smoothly at relatively small equatorial pitch angles ($\alpha_{eq} < 30°$), while the corresponding momentum diffusion rates tend to be zero as pitch angle decreases. For the electrons 100–400 keV (depending on L) near the loss cone, the pitch angle diffusion rates $\langle D_{\alpha\alpha} \rangle$ of exohiss can reach 5×10^{-5} s^{-1}, comparable to those of storm time plasmaspheric hiss. These numerical results suggest exohiss in the plasmatrough may potentially contribute to the slow decay of radiation belt ~< MeV electrons on a time scale of days. More statistical work is required to investigate the spatiotemporal distribution of exohiss, and the future radiation belt kinetic models may also need to include the effect of exohiss.

Acknowledgments

The Van Allen Probes data are available at the websites (http://emfisis.physics.uiowa.edu/Flight/ for EMFISIS and http://www.rbsp-ect.lanl.gov/data_pub/ for HOPE). This work was supported by the National Natural Science Foundation of China grants 41274169, 41274174, 41422405, 41174125, 41131065, 41121003, 41074120, 41231066, and 41304134, the Chinese Academy of Sciences grant KZCX2-EW-QN510 and KZZD-EW-01-4, and the National Key Basic Research Special Foundation of China grant 2011CB811403. This work was also supported from JHU/APL contracts 921647 and 967399 under NASA Prime contract NAS5-01072.

The Editor thanks two anonymous reviewers for their assistance in evaluating this paper.

References

Abel, B., and R. M. Thorne (1998a), Electron scattering loss in Earth's inner magnetosphere 1. Dominant physical processes, *J. Geophys. Res.*, *103*, 2385–2396, doi:10.1029/97JA02919.

Abel, B., and R. M. Thorne (1998b), Electron scattering loss in Earth's inner magnetosphere 2. Sensitivity to model parameters, *J. Geophys. Res.*, *103*, 2397–2408, doi:10.1029/97JA02920.

Bortnik, J., U. S. Inan, and T. F. Bell (2006), Landau damping and resultant unidirectional propagation of chorus waves, *Geophys. Res. Lett.*, *33*, L03102, doi:10.1029/2005GL024553.

Bortnik, J., R. M. Thorne, and N. P. Meredith (2007), Modeling the propagation characteristics of chorus using CRRES suprathermal electron fluxes, *J. Geophys. Res.*, *112*, A08204, doi:10.1029/2006JA012237.

Bortnik, J., R. M. Thorne, and N. P. Meredith (2008), The unexpected origin of plasmaspheric hiss from discrete chorus emissions, *Nature*, *452*, 62–66, doi:10.1038/nature06741.

Bortnik, J., W. Li, R. M. Thorne, V. Angelopoulos, C. Cully, J. Bonnell, O. Le Contel, and A. Roux (2009), An observation linking the origin of plasmaspheric hiss to discrete chorus emissions, *Science*, *324*, 775–778, doi:10.1126/science.1171273.

Chen, L., J. Bortnik, W. Li, R. M. Thorne, and R. B. Horne (2012a), Modeling the properties of plasmaspheric hiss: 1. Dependence on chorus wave emission, *J. Geophys. Res.*, *117*, A05201, doi:10.1029/2011JA017201.

Chen, L., J. Bortnik, W. Li, R. M. Thorne, and R. B. Horne (2012b), Modeling the properties of plasmaspheric hiss: 2. Dependence on the plasma density distribution, *J. Geophys. Res.*, *117*, A05202, doi:10.1029/2011JA017202.

Church, S. R., and R. M. Thorne (1983), On the origin of plasmaspheric hiss—Ray path integrated amplification, *J. Geophys. Res.*, *88*, 7941–7957, doi:10.1029/JA088iA10p07941.

Cornilleau-Wehrlin, N., J. Solomon, A. Korth, and G. Kremser (1985), Experimental study of the relationship between energetic electrons and ELF waves observed on board GEOS: A support to quasi-linear theory, *J. Geophys. Res.*, *90*, 4141–4154, doi:10.1029/JA090iA05p04141.

Denton, R. E., J. Goldstein, and J. D. Menietti (2002), Field line dependence of magnetospheric electron density, *Geophys. Res. Lett.*, *29*(24), 2205, doi:10.1029/2002GL015963.

Funsten, H. O., et al. (2013), Helium, Oxygen, Proton, and Electron (HOPE) mass spectrometer for the radiation belt storm probes mission, *Space Sci. Rev.*, *179*, 423–484, doi:10.1007/s11214-013-9968-7.

Glauert, S. A., and R. B. Horne (2005), Calculation of pitch angle and energy diffusion coefficients with the PADIE code, *J. Geophys. Res.*, *110*, A04206, doi:10.1029/2004JA010851.

Green, J. L., S. Boardsen, L. Garcia, W. W. L. Taylor, S. F. Fung, and B. W. Reinisch (2005), On the origin of whistler mode radiation in the plasmasphere, *J. Geophys. Res.*, *110*, A03201, doi:10.1029/2004JA010495.

Horne, R. B., R. M. Thorne, S. A. Glauert, J. M. Albert, N. P. Meredith, and R. R. Anderson (2005), Timescale for radiation belt electron acceleration by whistler mode chorus waves, *J. Geophys. Res.*, *110*, A03225, doi:10.1029/2004JA010811.

Kletzing, C. A., et al. (2013), The Electric and Magnetic Field Instrument Suite and Integrated Science (EMFISIS) on RBSP, *Space Sci. Rev.*, *179*, 127–181, doi:10.1007/s11214-013-9993-6.

Li, W., R. M. Thorne, J. Bortnik, Y. Nishimura, V. Angelopoulos, L. Chen, J. P. McFadden, and J. W. Bonnell (2010), Global distributions of suprathermal electrons observed on THEMIS and potential mechanisms for access into the plasmasphere, *J. Geophys. Res.*, *115*, A00J10, doi:10.1029/2010JA015687.

Li, W., et al. (2013), An unusual enhancement of low-frequency plasmaspheric hiss in the outer plasmasphere associated with substorm-injected electrons, *Geophys. Res. Lett.*, *40*, 3798–3803, doi:10.1002/grl.50787.

Li, W., et al. (2014), Quantifying hiss-driven energetic electron precipitation: A detailed conjunction event analysis, *Geophys. Res. Lett.*, *41*, 1085–1092, doi:10.1002/2013GL059132.

Lyons, L. R., and R. M. Thorne (1973), Equilibrium structure of radiation belt electrons, *J. Geophys. Res.*, *78*, 2142–2149, doi:10.1029/JA078i013p02142.

Mauk, B. H., N. J. Fox, S. G. Kanekal, R. L. Kessel, D. G. Sibeck, and A. Ukhorskiy (2013), Science objectives and rationale for the radiation belt storm probes mission, *Space Sci. Rev.*, *179*, 3–27, doi:10.1007/s11214-012-9908-y.

Meredith, N. P., R. B. Horne, R. M. Thorne, D. Summers, and R. R. Anderson (2004), Substorm dependence of plasmaspheric hiss, *J. Geophys. Res.*, *109*, A06209, doi:10.1029/2004JA010387.

Meredith, N. P., R. B. Horne, M. A. Clilverd, D. Horsfall, R. M. Thorne, and R. R. Anderson (2006), Origins of plasmaspheric hiss, *J. Geophys. Res.*, *111*, A09217, doi:10.1029/2006JA011707.

Mourenas, D., and J.-F. Ripoll (2012), Analytical estimates of quasi-linear diffusion coefficients and electron lifetimes in the inner radiation belt, *J. Geophys. Res.*, *117*, A01204, doi:10.1029/2011JA016985.

Ni, B., J. Bortnik, R. M. Thorne, Q. Ma, and L. Chen (2013), Resonant scattering and resultant pitch angle evolution of relativistic electrons by plasmaspheric hiss, *J. Geophys. Res. Space Physics*, *118*, 7740–7751, doi:10.1002/2013JA019260.

Ni, B., et al. (2014), Resonant scattering of energetic electrons by unusual low-frequency hiss, *Geophys. Res. Lett.*, *41*, 1854–1861, doi:10.1002/2014GL059389.

Russell, C. T., R. E. Holzer, and E. J. Smith (1969), OGO 3 observations of ELF noise in the magnetosphere: 1. Spatial extent and frequency of occurrence, *J. Geophys. Res.*, *74*, 755–777, doi:10.1029/JA074i003p00755.

Santolik, O., M. Parrot, and F. Lefeuvre (2003), Singular value decomposition methods for wave propagation analysis, *Radio Sci.*, *38*(1), 1010, doi:10.1029/2000RS002523.

Shprits, Y. Y., and B. Ni (2009), Dependence of the quasi-linear scattering rates on the wave normal distribution of chorus waves, *J. Geophys. Res.*, *114*, A11205, doi:10.1029/2009JA014223.

Sonwalkar, V. S., and U. S. Inan (1989), Lightning as an embryonic source of VLF hiss, *J. Geophys. Res.*, *94*, 6986–6994, doi:10.1029/JA094iA06p06986.

Su, Z., F. Xiao, H. Zheng, and S. Wang (2010), STEERB: A three-dimensional code for storm-time evolution of electron radiation belt, *J. Geophys. Res.*, *115*, A09208, doi:10.1029/2009JA015210.

Su, Z., et al. (2014), Nonstorm time dynamics of electron radiation belts observed by the Van Allen Probes, *Geophys. Res. Lett.*, *41*, 229–235, doi:10.1002/2013GL058912.

Summers, D. (2005), Quasi-linear diffusion coefficients for field-aligned electromagnetic waves with applications to the magnetosphere, *J. Geophys. Res.*, *110*, A08213, doi:10.1029/2005JA011159.

Summers, D., B. Ni, N. P. Meredith, R. B. Horne, R. M. Thorne, M. B. Moldwin, and R. R. Anderson (2008), Electron scattering by whistler-mode ELF hiss in plasmaspheric plumes, *J. Geophys. Res.*, *113*, A04219, doi:10.1029/2007JA012678.

Summers, D., Y. Omura, S. Nakamura, and C. A. Kletzing (2014), Fine structure of plasmaspheric hiss, *J. Geophys. Res. Space Physics*, *119*, 9134–9149, doi:10.1002/2014JA020437.

Thorne, R. M., E. J. Smith, R. K. Burton, and R. E. Holzer (1973), Plasmaspheric hiss, *J. Geophys. Res.*, *78*, 1581–1596, doi:10.1029/JA078i010p01581.

Thorne, R. M., S. R. Church, and D. J. Gorney (1979), On the origin of plasmaspheric hiss—The importance of wave propagation and the plasmapause, *J. Geophys. Res.*, *84*, 5241–5247, doi:10.1029/JA084iA09p05241.

Thorne, R. M., et al. (2013), Evolution and slow decay of an unusual narrow ring of relativistic electrons near L∼3.2 following the September 2012 magnetic storm, *Geophys. Res. Lett.*, *40*, 3507–3511, doi:10.1002/grl.50627.